Forward scattering of loaded and unloaded antennas

Gustafsson, Mats; Bach Andersen, Jørgen; Kristensson, Gerhard; Frølund Pedersen, Gert

2012

CODEN:LUTEDX/(TEAT-7217)/1-13/(2012)

Forward scattering of loaded and unloaded antennas

Mats Gustafsson, Jørgen Bach Andersen, Gerhard Kristensson, and Gert Frølund Pedersen

Electromagnetic Theory
Department of Electrical and Information Technology
Lund University
Sweden

Mats Gustafsson and Gerhard Kristensson
{mats.gustafsson,gerhard.kristensson}@eit.lth.se

Department of Electrical and Information Technology
Electromagnetic Theory
Lund University
P.O. Box 118
SE-221 00 Lund
Sweden

Jørgen Bach Andersen and Gert Frølund Pedersen
{jba,gfp}@es.aau.dk

Department of Electronic Systems
Aalborg University
Denmark

Editor: Gerhard Kristensson

Abstract

Forward scattering of antennas is related to antenna performance via the forward scattering sum rule. The forward scattering sum rule is an integral identity that shows that a weighted integral of the extinction cross section over all spectrum is proportional to the static polarizabiliy of the antenna structure. Here, the forward scattering sum rule is experimentally verified for loaded, short circuit, and open circuit cylindrical dipole antennas. It is also shown that the absorption efficiency cannot be greater than 1/2 for reciprocal linearly polarized lossless matched antennas with a symmetric radiation pattern.

1 Introduction

The interaction between an electromagnetic wave and a receiving antenna can be decomposed into absorption and scattering. The absorption properties are most important in the majority of antenna applications and they are also related to the radiation properties for reciprocal antennas [16]. There are also interests in the scattering of receiving antennas and it has been shown that the forward scattering sum rule is related to antenna properties such as bandwidth [8–10].

Investigations of antenna scattering goes back to the work by King [12], and its use to measure the input impedance has been investigated in [15, 20]. The analysis of minimum scattering antennas by Green in [5] shows that the scattering of small, single mode, and matched antennas scatter and absorb equal amounts of power. In [2], Andersen and Frandsen show that the absorption efficiency can take any number between zero and one. They also use forward scattering to introduce a bound on the absorption efficiency expressed in the scattering directivity. In [19], Steyskal considers absorption in large aperture antennas, and shows that a semi-transparent antenna is a requirement for an absorption efficiency greater than 1/2.

Forward scattering is particularly interesting as the forward scattered field is directly related the extinction cross section via the optical theorem. The forward scattering sum rule [6, 11, 18] shows that a weighted integral of the extinction cross section over all spectrum equals the static polarizabiliy of the scatterer times a constant. This provides a link between the static properties of the antenna structure and the dynamic properties of the antenna. It is used to derive physical bounds on resonance antennas in [8–10] and ultra-wideband antennas in [17].

In this paper, we determine the forward scattered field for loaded, short circuit, and open circuit dipole antennas experimentally. The results verify the forward scattering sum rule [6, 18]. They also show that loaded and short circuit antennas have equal integrated extinction, whereas the open circuit antenna has less. This is also understood from the polarizability as the open circuit corresponds to two separate cylinders, whereas the loaded and short circuit antennas correspond to a single cylinder. Moreover, it is shown that the geometrical average between the absorption cross sections in the forward and backward directions is bounded by the extinction cross section and the mismatch. In particular, it shows that matched an-

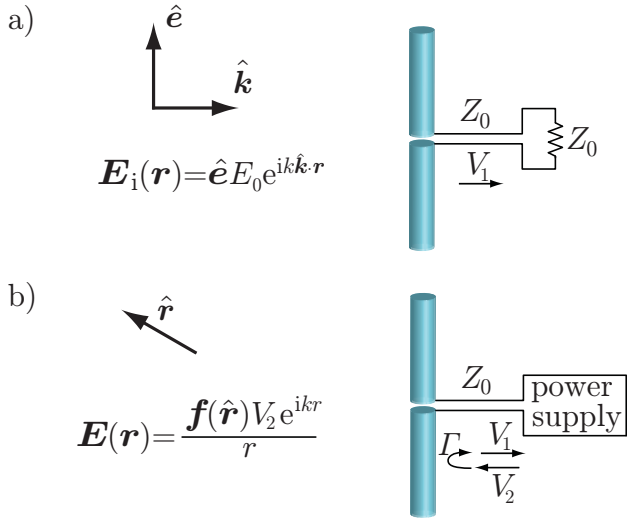

Figure 1: Receiving and transmitting antennas connected to a transmission line with characteristic impedance Z_0. a) receiving antenna with the incident field $\boldsymbol{E}_{\rm i}(\boldsymbol{r}) = \hat{\boldsymbol{e}}E_0{\rm e}^{{\rm i}k\hat{\boldsymbol{k}}\cdot\boldsymbol{r}}$, received voltage V_1, and a matched load. b) transmitting antenna with the incident voltage V_2, reflected voltage V_1, and radiated field $\boldsymbol{E}(\boldsymbol{r}) = \boldsymbol{f}(\hat{\boldsymbol{r}})V_2\frac{{\rm e}^{{\rm i}kr}}{r}$. The antenna is connected to a power supply that is matched to the transmission line.

tennas with a symmetric radiation patterns in the forward and backward directions cannot absorb more power than it scatters.

This paper is organized as follows. In Sec. 2, forward scattering of loaded and unloaded antennas are analyzed. Forward scattering measurements and the forward scattering sum rule are discussed in Secs 3 and 4, respectively. Experimental and numerical results for a cylindrical dipole are presented in Sec. 5. Conclusions are given in Sec. 6.

2 Antenna forward scattering

The interaction between an antenna and an electromagnetic wave can be decomposed into scattering and absorption. Consider an incoming linearly polarized plane wave $\boldsymbol{E}_{\rm i}(\boldsymbol{r}) = \hat{\boldsymbol{e}}E_0{\rm e}^{{\rm i}k\hat{\boldsymbol{k}}\cdot\boldsymbol{r}}$, where $\hat{\boldsymbol{k}}$ and $\hat{\boldsymbol{e}}$ are unit vectors describing the propagation direction and polarization, respectively, $\boldsymbol{r}$ the position vector, $k = \omega/{\rm c}_0$ the wavenumber, ${\rm c}_0$ the speed of light in vacuum, ${\rm i}^2 = -1$, and the time convention ${\rm e}^{-{\rm i}\omega t}$ is used. The scattered power, $P_{\rm s}$, is given by the scattering cross section, $\sigma_{\rm s}(\hat{\boldsymbol{k}}, \hat{\boldsymbol{e}})$, times the incident power flux $\mathcal{P}_{\rm in} = |E_0|^2/(2\zeta_0)$, *i.e.*, $P_{\rm s} = \sigma_{\rm s}\mathcal{P}_{\rm in}$, where ζ_0 denotes the free-space impedance. Similarly, the absorbed power is $P_{\rm a} = \sigma_{\rm a}\mathcal{P}_{\rm in}$, where $\sigma_{\rm a} = \sigma_{\rm a}(\hat{\boldsymbol{k}}, \hat{\boldsymbol{e}})$ is the absorption cross section.

The antenna is assumed to be lossless and connected to a lossless transmission line with characteristic impedance Z_0, see Fig. 1. Decompose the voltage in the transmission line into incident and reflected (or received) voltages V_2 and V_1, re-

spectively. Note that incident and reflected voltages refers to the antenna, *i.e.*, the incident voltage propagates from the power supply towards the antenna. They are related by the reflection coefficient of the antenna $\Gamma = (Z - Z_0)/(Z + Z_0)$, where Z is the antenna input impedance. The antenna is analyzed using incident plane waves and incident voltages.

To start, consider a receiving antenna with a load matched to the transmission line, see Fig. 1a. Conservation of power implies that the received power in the load equals the absorbed power for lossless antennas, *i.e.*,

$$\frac{|V_1|^2}{2Z_0} = \sigma_{\mathrm{a}} \mathcal{P}_{\mathrm{in}} = \frac{\sigma_{\mathrm{a}} |E_0|^2}{2\zeta_0} \tag{2.1}$$

that expresses the absorption cross section (partial effective aperture) as

$$\sigma_{\mathrm{a}}(\hat{\boldsymbol{k}}, \hat{\boldsymbol{e}}) = \frac{|V_1|^2 \zeta_0}{|E_0|^2 Z_0}. \tag{2.2}$$

Absorption and radiation properties are related to each other for reciprocal antennas. This offers an additional expression for the absorption cross section. Use that the radiated field is proportional to the incident voltage on the transmission line, V_2, and can be written as

$$\boldsymbol{E}(\boldsymbol{r}) = \boldsymbol{F}(\hat{\boldsymbol{r}}) \frac{\mathrm{e}^{\mathrm{i}kr}}{r} = \boldsymbol{f}(\hat{\boldsymbol{r}}) V_2 \frac{\mathrm{e}^{\mathrm{i}kr}}{r} \tag{2.3}$$

in an arbitrary direction $\hat{\boldsymbol{r}} = \boldsymbol{r}/r$ as $r = |\boldsymbol{r}| \to \infty$, see Fig 1b, where the far field $\boldsymbol{F}$ has dimension volt and $\boldsymbol{f}$ is dimensionless. The corresponding partial directivity [3] for the polarization $\hat{\boldsymbol{e}}$ is

$$D(\hat{\boldsymbol{r}}, \hat{\boldsymbol{e}}) = \frac{|\boldsymbol{f}(\hat{\boldsymbol{r}}) \cdot \hat{\boldsymbol{e}}|^2 4\pi}{\int |\boldsymbol{f}(\hat{\boldsymbol{r}})|^2 \, \mathrm{d}\Omega} = \frac{|\boldsymbol{f}(\hat{\boldsymbol{r}}) \cdot \hat{\boldsymbol{e}}|^2 4\pi Z_0}{\zeta_0 (1 - |\Gamma|^2)}, \tag{2.4}$$

where the integration in the denominator is over the unit sphere, and it is used that the total radiated power can be written

$$\frac{|V_2|^2 (1 - |\Gamma|^2)}{2Z_0} = \frac{|V_2|^2}{2\zeta_0} \int |\boldsymbol{f}(\hat{\boldsymbol{r}})|^2 \, \mathrm{d}\Omega. \tag{2.5}$$

The partial directivity in the direction $\hat{\boldsymbol{k}}$ is hence related to the absorption cross section (partial effective aperture) in the direction $-\hat{\boldsymbol{k}}$ via the relation [16]

$$\sigma_{\mathrm{a}}(-\hat{\boldsymbol{k}}, \hat{\boldsymbol{e}}) = \frac{D(\hat{\boldsymbol{k}}, \hat{\boldsymbol{e}})(1 - |\Gamma|^2)\pi}{k^2} = \frac{|\boldsymbol{f}(\hat{\boldsymbol{k}}) \cdot \hat{\boldsymbol{e}}|^2 Z_0 4\pi^2}{\zeta_0 k^2}. \tag{2.6}$$

It turns out that it is convenient to consider the geometric average between the absorption cross sections in the directions $\hat{\boldsymbol{k}}$ and $-\hat{\boldsymbol{k}}$. Combining the expressions (2.2) and (2.6) gives

$$\tilde{\sigma}_{\mathrm{a}}(\hat{\boldsymbol{k}}, \hat{\boldsymbol{e}}) = \sqrt{\sigma_{\mathrm{a}}(-\hat{\boldsymbol{k}}, \hat{\boldsymbol{e}}) \sigma_{\mathrm{a}}(\hat{\boldsymbol{k}}, \hat{\boldsymbol{e}})} = \left| \frac{\hat{\boldsymbol{e}} \cdot \boldsymbol{f}(\hat{\boldsymbol{k}}) V_1 2\pi}{k E_0} \right|. \tag{2.7}$$

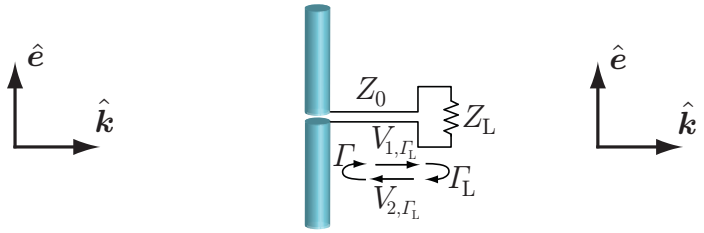

Figure 2: Antenna forward scattering. The antenna is connected to a transmission line with characteristic impedance Z_0 and electric length δ that is terminated in a load with impedance Z_{L}.

The above results are valid for arbitrary lossless antennas connected to a transmission line that is terminated in a matched load. We analyze the scattering and absorption properties of the antenna by terminating the transmission line of electric length δ in a load with impedance Z_{L}, giving the reflection coefficient $\Gamma_{\mathrm{L}} = (Z_{\mathrm{L}} - Z_0)/(Z_{\mathrm{L}} + Z_0)$, see Fig. 2. The scattering of this antenna can be decomposed into scattering from the antenna and scattering from the load that terminates the transmission line. The received voltage in the transmission line is $V_{1,0} = V_1$ in the case with a matched load $Z_{\mathrm{L}} = Z_0$. The received voltage is re-radiated if the transmission line is not terminated in a matched load. This part is given by

$$V_{2,\Gamma_{\mathrm{L}}} = V_1 \mathrm{e}^{\mathrm{i}2k\delta} \frac{\Gamma_{\mathrm{L}}}{1 - \mathrm{e}^{\mathrm{i}2k\delta}\Gamma_{\mathrm{L}}\Gamma} \tag{2.8}$$

and the re-radiated far field is $\boldsymbol{f}(\hat{\boldsymbol{r}})V_{2,\Gamma_{\mathrm{L}}}$.

The scattered far field, $\boldsymbol{F}_{\mathrm{s},\Gamma_{\mathrm{L}}}(\hat{\boldsymbol{r}})$, in the direction $\hat{\boldsymbol{r}}$ can be written as the sum

$$\boldsymbol{F}_{\mathrm{s},\Gamma_{\mathrm{L}}}(\hat{\boldsymbol{r}}) = \boldsymbol{F}_{\mathrm{s},0}(\hat{\boldsymbol{r}}) + \boldsymbol{f}(\hat{\boldsymbol{r}})V_1 \frac{\mathrm{e}^{\mathrm{i}2k\delta}\Gamma_{\mathrm{L}}}{1 - \mathrm{e}^{\mathrm{i}2k\delta}\Gamma_{\mathrm{L}}\Gamma}, \tag{2.9}$$

where $\boldsymbol{F}_{\mathrm{s},0}(\hat{\boldsymbol{r}})$ denotes the scattered far field with a matched load, *i.e.*, $\Gamma_{\mathrm{L}} = 0$ and $\boldsymbol{f}(\hat{\boldsymbol{r}})$ is the far field of the antenna normalized to a unit voltage excitation (2.3).

The extinction cross section σ_{ext} is the sum of the scattering and absorption cross sections, $\sigma_{\mathrm{ext}} = \sigma_{\mathrm{s}} + \sigma_{\mathrm{a}}$. The optical theorem [13, 18] shows that σ_{ext} is related to the forward scattered field as

$$\sigma_{\mathrm{ext},\Gamma_{\mathrm{L}}} = 4\pi \operatorname{Im}\left\{\frac{\hat{\boldsymbol{e}} \cdot \boldsymbol{F}_{\mathrm{s},\Gamma_{\mathrm{L}}}(\hat{\boldsymbol{k}})}{E_0 k}\right\} = \sigma_{\mathrm{ext},0} + 2\tilde{\sigma}_{\mathrm{a}} \operatorname{Im}\left\{\mathrm{e}^{\mathrm{i}\varphi}\frac{\mathrm{e}^{\mathrm{i}2k\delta}\Gamma_{\mathrm{L}}}{1 - \mathrm{e}^{\mathrm{i}2k\delta}\Gamma_{\mathrm{L}}\Gamma}\right\}, \tag{2.10}$$

where $\varphi = \arg(\hat{\boldsymbol{e}} \cdot \boldsymbol{f} V_1/E_0)$.

Use all reflection coefficients, $\mathrm{e}^{\mathrm{i}2k\delta}\Gamma_{\mathrm{L}}$, in (2.10) to show that the extinction cross section is bounded as

$$\begin{aligned} 0 \leq \min_{|\Gamma_{\mathrm{L}}|\leq 1} \sigma_{\mathrm{ext},\Gamma_{\mathrm{L}}} &= \sigma_{\mathrm{ext},0} + 2\tilde{\sigma}_{\mathrm{a}} \min_{|\xi|\leq 1} \operatorname{Im}\left\{\frac{\xi \mathrm{e}^{\mathrm{i}\varphi}}{1 - \Gamma\xi}\right\} \\ &= \sigma_{\mathrm{ext},0} - 2\tilde{\sigma}_{\mathrm{a}} \frac{1 + \operatorname{Im}\{\Gamma \mathrm{e}^{-\mathrm{i}\varphi}\}}{1 - |\Gamma|^2} \leq \sigma_{\mathrm{ext},0} - \frac{2\tilde{\sigma}_{\mathrm{a}}}{1 + |\Gamma|}, \end{aligned} \tag{2.11}$$

where the last inequality becomes an equality if $\arg\{\Gamma e^{-i\varphi}\} = -\pi/2$, see also App. A. The inequality (2.11) simplifies to a bound on the average absorption cross section

$$\tilde{\sigma}_a \leq \sigma_{ext,0} \frac{1+|\Gamma|}{2}. \tag{2.12}$$

Note that this shows that the absorption efficiency [2] of reciprocal lossless matched linearly polarized antennas with symmetric radiation patterns are bounded as $\eta = \sigma_a(k_0)/\sigma_{ext,0}(k_0) \leq 1/2$. A linearly polarized antenna can hence only have $\eta > 1/2$ if it is mismatched or if it has an unsymmetric radiation pattern. The bound (2.12) is of interest for cloaking of sensors [1], as it shows that it is difficult to reduce the scattering without mismatching the antenna.

It is noted that observations of $\boldsymbol{F}_{s,\Gamma_L}$ applied to different loads, Γ_L, can be used to determine $\tilde{\sigma}_a$ and Γ for the antenna. Use (2.9) and solve for σ_a and Γ. Here, we restrict the analysis to the cases with $\delta = 0$ and matched ($\Gamma_L = 0$), short ($\Gamma_L = -1$), and open ($\Gamma_L = +1$) circuit loads. This gives

$$\begin{cases} \Delta_s = 4\pi \hat{\boldsymbol{e}} \cdot (\boldsymbol{F}_{s,-1} - \boldsymbol{F}_{s,0})/(kE_0) = \frac{-2\tilde{\sigma}_a e^{i\varphi}}{1+\Gamma} \\ \Delta_o = 4\pi \hat{\boldsymbol{e}} \cdot (\boldsymbol{F}_{s,+1} - \boldsymbol{F}_{s,0})/(kE_0) = \frac{2\tilde{\sigma}_a e^{i\varphi}}{1-\Gamma} \end{cases} \tag{2.13}$$

for the open and short circuit cases, respectively, with the solution

$$\tilde{\sigma}_a = \left| \frac{\Delta_s \Delta_o}{\Delta_s - \Delta_o} \right| \quad \text{and } \Gamma = \frac{\Delta_o + \Delta_s}{\Delta_o - \Delta_s}. \tag{2.14}$$

The input impedance is also determined to $Z = -Z_0 \Delta_o/\Delta_s$. These results are related to the common backscattering technique [12, 15, 20].

3 Forward scattering measurement

It is not possible to measure the forward scattered field directly. Instead, the scattered field is determined from the difference between the measured fields with and without the scattering object present. This requires a high signal to noise ratio as the incident field dominates over the scattered field.

The measurement setup for the forward scattered field is illustrated in Fig. 3. The transmitting and receiving antennas faces each other at the distance $2d$. First, the co-polarized field, $E_{r,0}$, without the scatterer present is recorded. The scatterer (AUT) is placed in the center between the transmitting and receiving antennas and the co-polarized field $E_{r,s}$ is recorded. The scattered field at the receiving antenna is $E_s = E_{r,s} - E_{r,0}$. Use the far-field approximation to estimate the incident field at the scattering object. The electric field at the distance r from the transmitter is written $E(r) = V_0 e^{ikr}/r$, where the voltage V_0 quantifies the amplitude of the transmitted field. The incident field at the scattering object is $E_0 = E(d) = V_0 e^{ikd}/d$ and the received field without the scattering object is $E_{r,0} = E(2d) = V_0 e^{i2kd}/(2d)$ giving

$$E_0 = 2E_{r,0} e^{-ikd}. \tag{3.1}$$

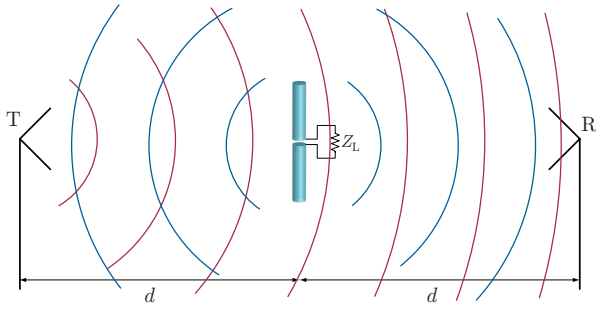

Figure 3: Forward scattering setup. A spherical wave from the transmitter (T) illuminates the antenna under test (AUT) and the receiver (R). It induces a spherical wave originating from the AUT.

The far-field approximation is used to express the scattered far-field in the received scattered field, *i.e.*,

$$E_\mathrm{s} = F_\mathrm{s}\frac{\mathrm{e}^{\mathrm{i}kd}}{d} \quad \text{and } F_\mathrm{s} = d\mathrm{e}^{-\mathrm{i}kd}E_\mathrm{s}. \tag{3.2}$$

Finally, the optical theorem [13, 18] is used to determine the extinction cross section from the forward scattered field as $\sigma_\mathrm{ext} = \operatorname{Im} h$, where

$$h = 4\pi\frac{F_\mathrm{s}}{kE_0} = \frac{2\pi d}{k}\left(\frac{E_\mathrm{r,s}}{E_\mathrm{r,0}} - 1\right). \tag{3.3}$$

4 Forward scattering sum rule

Causality implies that $h(k)$ is a holomorphic function of k for $\operatorname{Im} k > 0$, see [6, 9, 18]. This together with the sign $\operatorname{Im} h(k) \geq 0$ classifies $h(k)$ as a Herglotz function [4, 14]. The low-frequency asymptotic behavior, $h \sim \gamma k + \mathcal{O}(k^2)$, where

$$\gamma = \hat{\boldsymbol{e}} \cdot \boldsymbol{\gamma}_\mathrm{e} \cdot \hat{\boldsymbol{e}} + (\hat{\boldsymbol{k}} \times \hat{\boldsymbol{e}}) \cdot \boldsymbol{\gamma}_\mathrm{m} \cdot (\hat{\boldsymbol{k}} \times \hat{\boldsymbol{e}}) \tag{4.1}$$

and $\boldsymbol{\gamma}_\mathrm{e}$ and $\boldsymbol{\gamma}_\mathrm{m}$ are the electro- and magneto-static polarizability dyadics, respectively, and the high-frequency asymptotic [6, 11] are used to show that $\sigma_\mathrm{ext} = \operatorname{Im} h$ satisfies the forward scattering sum rule [4, 6, 9, 18]

$$\frac{2}{\pi}\int_0^\infty \frac{\sigma_\mathrm{ext}(k; \hat{\boldsymbol{k}}, \hat{\boldsymbol{e}})}{k^2}\,\mathrm{d}k = \gamma. \tag{4.2}$$

The integral (4.2) is employed in various ways to produce bounds for different antenna applications, *e.g.*, resonant and constant partial-realized gain in [8–10] and ultra-wide band cases in [17].

5 Cylindrical dipoles

The forward scattering is illustrated for short circuit, open circuit, and loaded dipole antennas. The short circuit dipole is made of a cylindrical copper wire with diam-

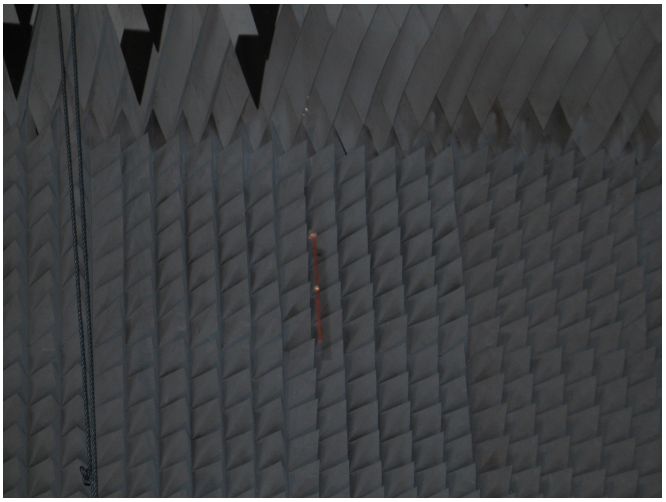

Figure 4: The dipole used during the measurements.

eter $d = 3.57\,\mathrm{mm}$ and length $\ell \approx 150\,\mathrm{mm}$. The open circuit and (loaded) dipoles are composed of two cylinders with lengths 73.7 mm and 73.5 mm (74.2 mm and 74.4 mm), respectively, separated by a 1.1 mm gap. A 50Ω lumped resistance is placed between the cylinders for the loaded dipole.

The measurements are conducted in the anechoic room at Aalborg University, which is $7 \times 7 \times 10\,\mathrm{m}^3$. An Emco 3115 horn antenna is used as the transmitting antenna, and a dual polarized horn from ETS, located approximately 5.5 m from the transmitting horn, is used for receiving. The antenna under investigation is centered in the room and fixed by a thin fishing line attached to the ceilings. Altogether 3 dipoles are measured — one which is loaded with $50\,\Omega$, one open and one shorted, see Fig 4.

The forward scattered field is measured as described in Sec. 3 and simulated using the method of moments (MoM). The real and imaginary parts of h are depicted in Figs 5, 6, and 7 for the loaded, short circuit, and open circuit dipoles, respectively. It is observed that the resonance frequencies of the short circuit and loaded dipoles are around 0.9 GHz whereas the resonance for the opens circuit dipole is at 1.5 GHz. The linear low-frequency asymptotic behavior, $h = \gamma k + \mathcal{O}(k^2)$, is also noted in the figures. Moreover, it is seen that the proportionally constants, γ, are similar for the short circuit and loaded dipoles and smaller for the open circuit dipole. The difference between the low-frequency asymptotic behavior of $\sigma_{\mathrm{ext}} = \mathrm{Im}\, h$ for the loaded and short and open circuit dipoles can also be seen, *i.e.*, $\sigma_{\mathrm{a}} \approx 0$ for the open and short circuit dipoles giving $\sigma_{\mathrm{ext}} = \mathcal{O}(k^4)$ as $k \to 0$.

The integrated extinction in (4.2) is also determined: loaded $644\,\mathrm{cm}^3$, short circuit $644\,\mathrm{cm}^3$, and open circuit $265\,\mathrm{cm}^3$ for the numerical data in $0 < f \leq 6\,\mathrm{GHz}$, see Tab. 1. The corresponding measured data gives: loaded $605\,\mathrm{cm}^3$, short circuit $670\,\mathrm{cm}^3$, and open circuit $322\,\mathrm{cm}^3$, where the frequency interval $0.5\,\mathrm{GHz} \leq f \leq 6\,\mathrm{GHz}$ is used. Note that the weight factor k^{-2} in (4.2) makes that experimental data very sensitive to noise at low frequencies.

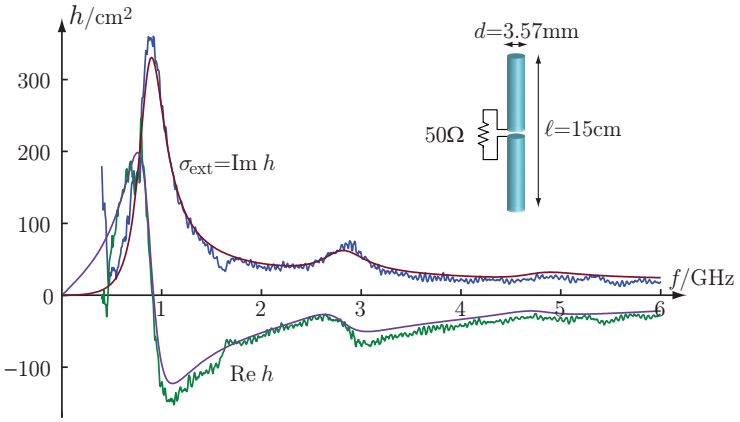

Figure 5: Measured (rough curves) and simulated (smooth curves) forward scattering of a 50Ω loaded cylindrical dipole antenna with lengths $\ell_1 = 74.2\,\text{mm}$ and $\ell_2 = 74.4\,\text{mm}$, diameters $d = 3.57\,\text{mm}$ and separation 1.1 mm.

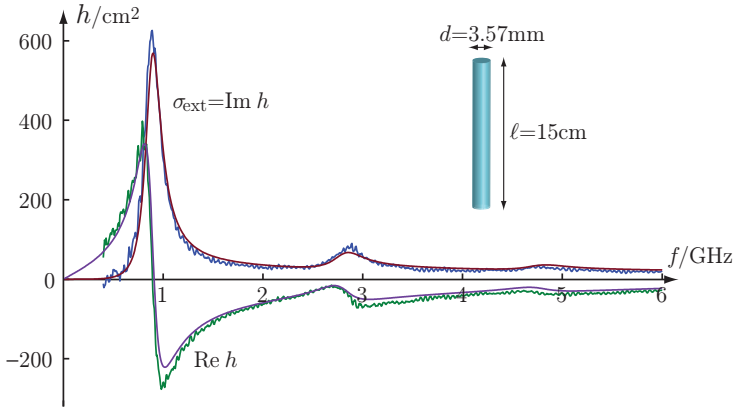

Figure 6: Measured (rough curves) and simulated (smooth curves) forward scattering of a cylinder with length $\ell = 150\,\text{mm}$ and diameter $d = 3.57\,\text{mm}$.

The polarizabilities of the dipoles are determined by the separation of charge for the antenna structures placed in an external, homogeneous electrostatic field using the MoM[1] [7]. The equipotential surfaces of the external electric field parallel with the dipoles, *i.e.*, $\boldsymbol{E} = E_0\hat{\boldsymbol{z}}$, are depicted in Fig. 8. It is observed that the short circuit and loaded antennas are similar in the static limit, *i.e.*, the resistive load that connects the cylinders produces a single object with constant potential. The open circuit dipole is divided into two cylinders with different potentials. The numerical values are $\gamma = \hat{\boldsymbol{z}} \cdot \boldsymbol{\gamma}_\text{e} \cdot \hat{\boldsymbol{z}} \approx 661\,\text{cm}^3$ for the solid cylinder and $\gamma \approx 291\,\text{cm}^3$ for the two cylinders.

The forward scattering data for the loaded (Fig. 5), short- (Fig. 6), and open-circuit (Fig. 7) dipoles are used to determine the absorption cross section and re-

[1] see also http://www.mathworks.com/matlabcentral/fileexchange/26806-antennaq

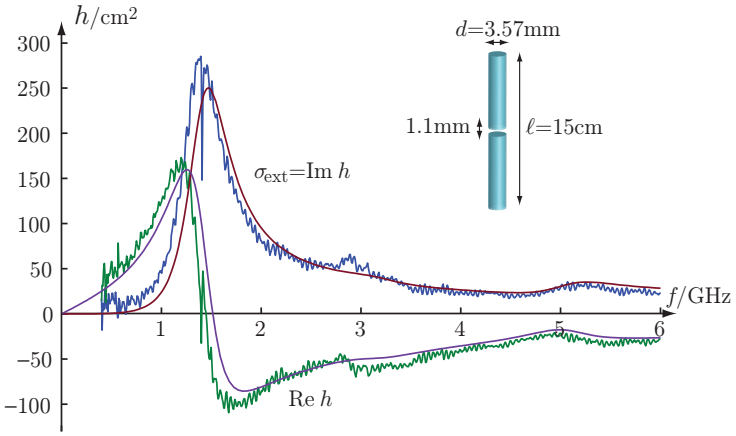

Figure 7: Measured (rough curves) and simulated (smooth curves) forward scattering of two cylinders with lengths $\ell_1 = 73.7\,\mathrm{mm}$ and $\ell_2 = 73.5\,\mathrm{mm}$, diameters $d = 3.57\,\mathrm{mm}$ and separation $1.1\,\mathrm{mm}$.

		loaded	short	open
simulation:	$\gamma/\,\mathrm{cm}^3$	661	661	291
simulation:	$\frac{2}{\pi}\int_0^{k_2} \frac{\sigma_{\mathrm{ext}}(k)}{k^2}\,\mathrm{d}k/\,\mathrm{cm}^3$	644	644	265
measurement:	$\frac{2}{\pi}\int_{k_1}^{k_2} \frac{\sigma_{\mathrm{ext}}(k)}{k^2}\,\mathrm{d}k/\,\mathrm{cm}^3$	605	670	322

Table 1: Numerical and experimental results for the loaded, short-, and open circuit dipole antennas. The simulations and measurements are for $0 \le f \le 6\,\mathrm{GHz}$ and $0.5 \le f \le 6\,\mathrm{GHz}$, respectively.

flection coefficient for the loaded antenna through the relation (2.14). The resulting absorption cross section is depicted in Fig. 9. It is observed that the measured and simulated results are similar. The absorption cross section is maximal for $f_0 \approx 0.9\,\mathrm{GHz}$ with $\sigma_{\mathrm{a}}(f_0) \approx 160\,\mathrm{cm}^2$. This is approximately half of the extinction cross section depicted in Fig. 5. The corresponding reflection coefficient is depicted in Fig. 10. Here, it is seen that the antenna is not perfectly matched at $f_0 \approx 0.9\,\mathrm{GHz}$. A matched dipole has a radiation resistance close to $74\,\Omega$ and not $50\,\Omega$ as is used here. It is also observed that the reflection coefficient is close to one for $f \ll f_0$. The simulated and measured results show similar features, but the noise increases compared to the forward scattering results in Figs 5, 6, and 7.

The absorption efficiency $\eta = \sigma_{\mathrm{a}}/\sigma_{\mathrm{ext}}$ is depicted in Fig. 11. Here, it is observed that $\eta(f_0) \approx 0.45$ and $\eta(f) \approx 1$ for $f \ll f_0$. This is in agreement with the results in (2.12) as the dipole antenna is mismatched. The dipole acts as a probe in the frequency range $f \ll f_0$.

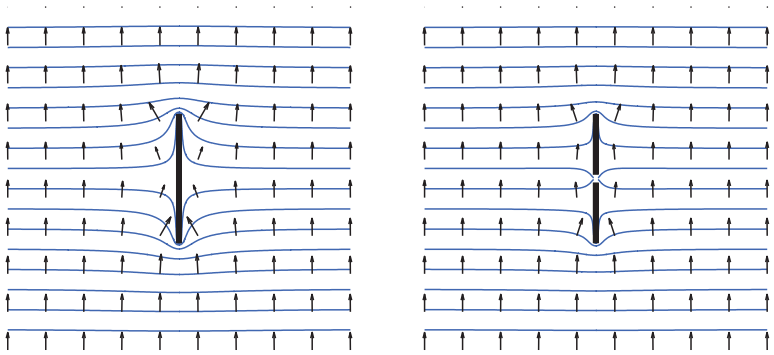

Figure 8: Equipotential surfaces and electric field lines for the short circuit and loaded dipoles (left) and open circuit dipole (right).

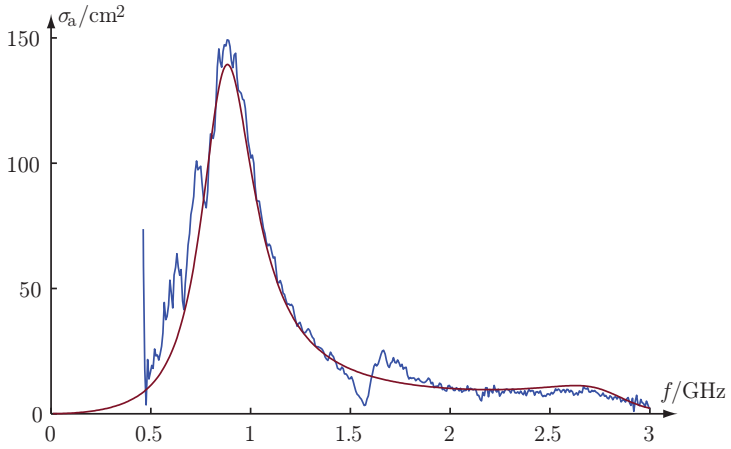

Figure 9: Measured (rough curves) and simulated (smooth curves) absorption cross sections, σ_a, for the loaded dipole antenna as determined from (2.14).

6 Conclusions

An experimental verification of the forward scattering sum rule for loaded, short circuit, and open circuit cylindrical dipole antennas is presented. The experimental results agree well with the MoM simulations. The integrated extinction [6, 18] is within 10% from the electrostatic polarizability. Moreover, it is shown that the combination of the loaded, short circuit, and open circuit antennas can be used to determine the input impedance and the average of the absorption cross sections in the forward and backward directions. We also use the optical theorem to show a bound on the absorption efficiency of linearly polarized antennas. In particular, it shows that matched antennas with a symmetric radiation pattern cannot have an absorption efficiency greater than 1/2.

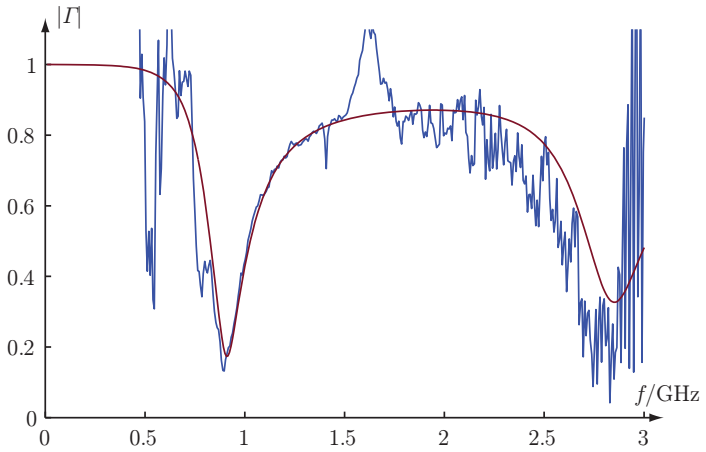

Figure 10: Measured (rough curves) and simulated (smooth curves) reflection coefficients, $|\Gamma|$, for the loaded dipole antenna determined using (2.14).

Appendix A An inequality

The second equality in (2.11) is analyzed using the map $\xi \to g_1(\xi) = \xi/(1-\xi z)$ of the unit circle $|\xi| \leq 1$, where $z = \mathrm{e}^{-\mathrm{i}\phi}\Gamma$ and $|z| < 1$. This is a conformal map mapping circles into circles. Hence, it is first observed that $\min \mathrm{Im}\{g_1(\xi)\}$ is at the boundary $|\xi| = 1$. This simplifies the problem to minimization of $\min_{|\xi|=1} \mathrm{Im}\,\{g_2(\xi)\}$, where $g_2(\xi) = 1/(\xi - z)$. We also note that the final inequality in (2.11) can be easily derived using the specific value $\xi = x + \mathrm{i}\sqrt{1-x^2}$, where $x = \mathrm{Re}\{z\}$ giving

$$\min_{|\xi|=1} \mathrm{Im}\left\{\frac{1}{\xi - z}\right\} \leq \mathrm{Im}\left\{\frac{1}{\mathrm{i}\sqrt{1-x^2} - \mathrm{i}y}\right\}$$
$$= \frac{-1}{\sqrt{1-x^2} - y} \leq \frac{-1}{1 + \sqrt{x^2+y^2}} = \frac{-1}{1+|z|}. \quad \text{(A.1)}$$

References

[1] A. Alù and N. Engheta. Cloaking a sensor. *Physical review letters*, **102**(23), 233901, 2009.

[2] J. B. Andersen and A. Frandsen. Absorption efficiency of receiving antennas. *IEEE Trans. Antennas Propagat.*, **53**(9), 2843–2849, 2005.

[3] Antenna Standards Committee of the IEEE Antennas and Propagation Society. IEEE Standard Definitions of Terms for Antennas, 1993. IEEE Std 145-1993.

[4] A. Bernland, A. Luger, and M. Gustafsson. Sum rules and constraints on passive systems. *J. Phys. A: Math. Theor.*, **44**(14), 145205, 2011.

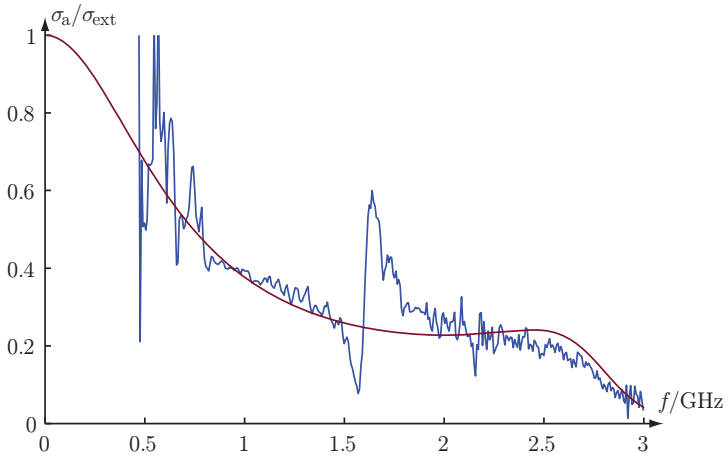

Figure 11: Measured (rough curves) and simulated (smooth curves) absorption efficiencies, σ_a/σ_{ext}, for the loaded dipole antenna using Fig. 5. and Fig. 9.

[5] R. Green. Scattering from conjugate-matched antennas. *IEEE Trans. Antennas Propagat.*, **14**(1), 17–21, 1966.

[6] M. Gustafsson. Time-domain approach to the forward scattering sum rule. *Proc. R. Soc. A*, **466**, 3579–3592, 2010.

[7] M. Gustafsson. Physical bounds on antennas of arbitrary shape. In *Antennas and Propagation Conference (LAPC), 2011 Loughborough*, pages 1–5. IEEE, 2011.

[8] M. Gustafsson, M. Cismasu, and S. Nordebo. Absorption efficiency and physical bounds on antennas. *International Journal of Antennas and Propagation*, (Article ID 946746), 1–7, 2010.

[9] M. Gustafsson, C. Sohl, and G. Kristensson. Physical limitations on antennas of arbitrary shape. *Proc. R. Soc. A*, **463**, 2589–2607, 2007.

[10] M. Gustafsson, C. Sohl, and G. Kristensson. Illustrations of new physical bounds on linearly polarized antennas. *IEEE Trans. Antennas Propagat.*, **57**(5), 1319–1327, May 2009.

[11] M. Gustafsson, I. Vakili, S. E. B. Keskin, D. Sjöberg, and C. Larsson. Optical theorem and forward scattering sum rule for periodic structures. *IEEE Trans. Antennas Propagat.*, **60**(8), 3818–3826, 2012.

[12] D. King. The measurement and interpretation of antenna scattering. *Proceedings of the IRE*, **37**(7), 770–777, 1949.

[13] R. G. Newton. *Scattering Theory of Waves and Particles*. Springer-Verlag, New York, 1982.

[14] H. M. Nussenzveig. *Causality and dispersion relations.* Academic Press, London, 1972.

[15] P. Pursula, M. Hirvonen, K. Jaakkola, and T. Varpula. Antenna effective aperture measurement with backscattering modulation. *IEEE Trans. Antennas Propagat.*, **55**(10), 2836–2843, 2007.

[16] S. Silver. *Microwave Antenna Theory and Design*, volume 12 of *Radiation Laboratory Series.* McGraw-Hill, New York, 1949.

[17] C. Sohl and M. Gustafsson. A priori estimates on the partial realized gain of Ultra-Wideband (UWB) antennas. *Quart. J. Mech. Appl. Math.*, **61**(3), 415–430, 2008.

[18] C. Sohl, M. Gustafsson, and G. Kristensson. Physical limitations on broadband scattering by heterogeneous obstacles. *J. Phys. A: Math. Theor.*, **40**, 11165–11182, 2007.

[19] H. Steyskal. On the power absorbed and scattered by an antenna. *IEEE Antennas and Propagation Magazine*, **52**(6), 41 –45, 2010.

[20] W. Wiesbeck and E. Heidrich. Wide-band multiport antenna characterization by polarimetric RCS measurements. *IEEE Trans. Antennas Propagat.*, **46**(3), 341–350, 1998.